Bimodal diffusion in power-law shear flows

E. Ben-Naim and S. Redner
Center for Polymer Studies, Boston University, Boston, Massachusetts 02215
and Department of Physics, Boston University, Boston, Massachusetts 02215

D. ben-Avraham
Department of Physics, Clarkson University, Potsdam, New York 13699
(Received 14 November 1991)

The motion of dynamically neutral Brownian particles that are influenced by a unidirectional velocity field of the form $\mathbf{v}(x,y)=v_0|y|^{\beta}\mathrm{sgn}(y)\hat{\mathbf{x}}$, with $\beta\geq 0$, is studied. Analytic expressions for the two-dimensional probability distribution are obtained for the special cases $\beta=0$ and 1. As a function of β, the longitudinal probability distribution of displacements exhibits bimodality for $\beta<\beta_c$ and unimodality otherwise. A simple effective-velocity approximation is introduced that provides an integral form for the longitudinal probability distribution for general β and predicts the existence of this transition. A numerical exact enumeration of the probability distribution yields $\beta_c=\frac{3}{4}$. The power-law model parallels the behavior found for tracer motion in a class of non-Newtonian fluids, where a unimodal-to-bimodal transition is also found to occur.

PACS number(s): 47.15.−x, 47.50.+d, 05.40.+j, 02.50.+s

I. INTRODUCTION

The phenomenon in which a Brownian particle moves faster than diffusively arises in a number of diverse situations. In the context of fluid mechanics [1–3], for example, a dynamically neutral tracer particle in a linear shear flow with fluid velocity $\mathbf{v}(x,y)\propto y\hat{\mathbf{x}}$ exhibits a mean-square longitudinal displacement that grows in time as $\langle x(t)^2\rangle\sim t^3$. It is also well known that the probability distribution of longitudinal displacements for the tracer particles is Gaussian, $P_L(x,t)\equiv\int P(x,y,t)dy \sim\exp(\mathrm{const}\times x^2/t^3)$. In the context of random media, enhanced diffusion can arise when there is a steady unidirectional convection field whose magnitude depends stochastically on the transverse coordinate [4,5]. One such example is a system where the magnitude of the longitudinal velocity is itself determined by a random walk [6]. In a typical realization of this "random-walk" shear flow, the longitudinal velocity at transverse coordinate y increases as $y^{1/2}$, a feature that leads to faster-than-ballistic motion of a tracer particle. The competition between transverse mixing and the large effective longitudinal steps imposed by the flow field also leads to a *bimodal* form for $P_L(x,t)$ in a single random-shear-flow configuration. This intriguing aspect of the system motivates our present work.

In this paper, we investigate the motion of a dynamically neutral tracer particle that moves in a deterministic velocity field $\mathbf{v}(x,y)=v_0|y|^{\beta}\mathrm{sgn}(y)\hat{\mathbf{x}}$ (Fig. 1). This can be viewed as the average over many configurations of the random-walk shear-flow problem. We find, rather strikingly, that the probability distribution of longitudinal displacements exhibits a transition from unimodal to bimodal behavior as β is varied. One of our primary goals is to clarify this phenomenon. A potential application of this result is that power-law shear flow qualitatively mimics the flow field of a non-Newtonian fluid under fixed external shear. In this latter system, we have also found that there is a transition from a unimodal to a bimodal probability distribution when the flow condition of the fluid is varied. Thus the shape of $P_L(x,t)$ may provide useful information about the flow field of the ambient fluid.

In Sec. II, we discuss some basic scaling properties of $P_L(x,t)$ in power-law shear flow. The exact solutions for the full two-dimensional probability distribution in the special cases of $\beta=0$ and 1 are then presented in Secs. III and IV. In the case of "split flow," $\beta=0$, our solution represents the extension of the classical arcsine law [7], which is equivalent to the distribution of longitudinal displacements, to the full distribution in the plane. We then

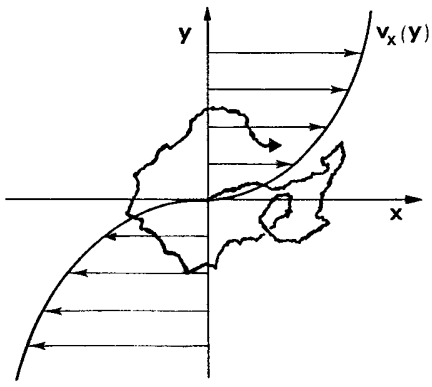

FIG. 1. Velocity profile of power-law shear flow and a schematic illustration of the trajectory of a dynamically neutral Brownian particle in this flow field.

describe an alternate way of obtaining the probability distribution for the case of linear shear flow, $\beta=1$. While the exact solution in the continuum limit is well known [1–3], our simple approach for the discrete case clearly exhibits the connection between Brownian motion in linear shear flow and a temporally inhomogeneous diffusion process, where the diffusion coefficient grows as t^2. In Sec. V, we present an effective-velocity approximation for writing $P_L(x,t)$ for general β, which predicts a unimodal-to-bimodal transition at $\beta=\frac{8}{9}$. In Sec. VI, numerical results from exact enumeration are given that suggest that the critical value of β is $\frac{3}{4}$. In Sec. VII, we present exact enumerations for the qualitatively similar problem of tracer motion in the flow field of a non-Newtonian fluid under a constant external shear stress. A unimodal-to-bimodal transition is again found as the flow conditions of the fluid are varied.

II. SCALING PROPERTIES

For a fluid in which the flow field is $\mathbf{v}(x,y)=v_0|y|^\beta \mathrm{sgn}(y)\hat{\mathbf{x}}$, the probability distribution of an immersed dynamically neutral Brownian particle obeys the convection-diffusion equation

$$\frac{\partial P(x,y,t)}{\partial t}+\mathrm{sgn}(y)|y|^\beta v_0\frac{\partial P(x,y,t)}{\partial x}=D\frac{\partial^2 P(x,y,t)}{\partial y^2}\ , \quad (1)$$

where the subdominant contribution of diffusion in the longitudinal (x) direction has been neglected at the outset. Our primary goal is to determine the distribution of longitudinal displacements, $P_L(x,t)\equiv\int P(x,y,t)dy$, with the initial conditions $P(\mathbf{r},t=0)=\delta(\mathbf{0})$. The transverse displacement behaves in a purely diffusive manner, $y\sim\sqrt{Dt}$, as can immediately be confirmed by integration of Eq. (1) over x. On the other hand, the root-mean-square longitudinal displacement $x_{\rm rms}$ may be roughly estimated by noting that the longitudinal velocity at time t is $v_x(y(t))\sim v_0(Dt)^{\beta/2}$. Consequently,

$$x_{\rm rms}\sim(v_0 t)(Dt)^{\beta/2}\ , \quad (2)$$

with the correlation-length exponent $\nu=1+\beta/2$. The increase in longitudinal velocity with time scale is the underlying mechanism that leads to $x_{\rm rms}$ growing faster than linearly with time. It is interesting to notice that, for $\beta=0$, x is independent of the diffusion coefficient D.

For describing the probability distribution, it will be convenient to introduce the scaled longitudinal and transverse displacements,

$$\xi=x/(v_0 t)(Dt)^{\beta/2},\quad \eta=y/\sqrt{Dt}\ , \quad (3)$$

respectively. In terms of these scaled variables, we may also write the probability distribution in the following convenient scaling form:

$$f(\xi,\eta)\equiv(v_0 t)(Dt)^{(1+\beta)/2}P(x,y,t)\ . \quad (4)$$

From this, we also define the scaled form of the longitudinal probability distribution as $f_L(\xi)\equiv\int f(\xi,\eta)d\eta$. We expect that this function has the asymptotic behaviors $f_L(\xi)\to$const as $\xi\to 0$, and $f_L(\xi)\sim e^{-\xi^\delta}$, as $\xi\to\infty$. We can immediately deduce the value of the large-distance shape exponent δ by constructing a rough estimate for the probability of finding the extreme walks that contribute to the tail of the distribution [8,9]. For power-law shear flow, the most longitudinally stretched walk must have each transverse step in the same direction, in order that the walk has the largest possible velocity at each time step. This implies that the probability of finding a stretched walk decays as a pure exponential in t, $e^{-\alpha t}$. On the other hand, a stretched walk has a longitudinal displacement, which scales as $x_{\max}(t)\sim\int^t y^\beta dy\sim t^{1+\beta}$. This maximal value corresponds to a scaled displacement $\xi\sim t^{\beta/2}$, and correspondingly, $f_L(\xi)\sim\exp(-t^{\delta\beta/2})$. Since we have argued that this probability decays as a pure exponential in t, we conclude that $\delta=2/\beta$. Using $\nu=1+\beta/2$, the expression for δ can be written as $\delta=|1-\nu|^{-1}$. This is of the same form as the classical Fisher relation [10] between the shape and size exponents $\delta=(1-\nu)^{-1}$ for the usual situation where $\nu<1$.

III. SPLIT FLOW

In this section we present an exact solution for the two-dimensional probability distribution of displacements in the case of "split flow," where the velocity field is $\mathbf{v}(x,y)=v_0\mathrm{sgn}(y)\hat{\mathbf{x}}$ (Fig. 2). Within a discrete version of the problem, the transverse behavior is simply a symmetric random walk, while the longitudinal displacement is proportional to the difference n_+-n_-, where n_+ and n_- are the number of steps that the transverse random walk spends in the upper and lower half planes, respectively. Since n_++n_- equals the total number of steps n, the probability distribution in the plane can be found once we determine $\mathcal{P}_n(y,n_+)$, the probability that an n-step random walk is at transverse position y and has spent exactly n_+ steps in the upper half plane.

Consider first the special case of $\mathcal{P}_n(y=0,n_+)$, the probability that an n-step walk, which starts and ends at $y=0$, spends n_+ steps in the upper half plane. Rather surprisingly, this probability is *independent* of n_+ [7],

$$\mathcal{P}_n(y=0,n_+)\sim(1/2\pi n^3)^{1/2}\ . \quad (5)$$

To obtain the corresponding probability for arbitrary y, it is helpful to visualize the individual random paths that contribute to this probability as the sequence of points

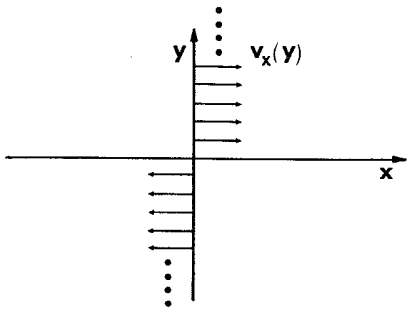

FIG. 2. Velocity profile of split flow.

$\{i,y_i\}$ in a space-time representation (Fig. 3). For a walk that starts at $\{0,0\}$ and ends at $\{n,y_n\}$ there will be a "break point," which is the last time that the walk passes through the axis $y=0$. Without loss of generality, we need only consider the case $y_n>0$. We define the break point to occur at time step $n-k$, and divide the trajectory from $\{0,0\}$ to $\{n,y_n\}$ into a "return" segment from $\{0,0\}$ to $\{n-k,0\}$ and a "first-passage" segment from $\{n-k,0\}$ to $\{n,y_n\}$. The probability for the full trajectory can then be computed as the convolution of the probabilities of these two segments.

The initial return segment takes $n-k$ steps, and by construction n_+-k of these lie in the upper half plane. Consequently, the probability for this segment is $\mathcal{P}_{n-k}(y=0,n_+-k)$. By construction, the subsequent k-step segment touches $y=0$ only once. Hence the transverse coordinate of the time-reversed segment is exactly a k-step first-passage trajectory from $y=y_n$ to $y=0$, and the probability for this event is [7]

$$f_k(y)\sim y(2/\pi k^3)^{1/2}\exp(-y^2/2k)\ . \tag{6}$$

The convolution of these two probabilities yields

$$\mathcal{P}_n(y,n_+)=\sum_{k=y}^{n_+}\mathcal{P}_{n-k}(0,n_+-k)f_k(y)$$
$$\sim\int_{k=y}^{n_+}dk\frac{y}{\pi[k(n-k)]^{3/2}}e^{-y^2/2k}\ . \tag{7}$$

The lower limit of k is y, since the walker must spend at least y steps in the first-passage segment of the trajectory in order to reach transverse position y. Changing variables to $u=y^2/2k$, defining $x=v_0(n_+-n_-)$, and replacing n by t, the integral can be performed to give

$$f(\xi,\eta)\sim\frac{1-\eta^2}{\sqrt{2\pi}}\operatorname{erfc}\left[\eta\left[\frac{1-\xi}{2(1+\xi)}\right]^{1/2}\right]e^{-\eta^2/2}$$
$$+\frac{\eta}{\pi}\left[\frac{1+\xi}{1-\xi}\right]^{1/2}e^{-\eta^2/1+\xi}\ , \tag{8}$$

where ξ and η are the scaled longitudinal and transverse coordinates defined in Eq. (3) (note that $|\xi|<1$).

It is instructive to examine the asymptotic behaviors of this probability distribution. Consider first the behavior of longitudinal slices, i.e., fix η and vary ξ. For $\eta\ll1$ and $-1+2\eta^2<\xi<1$, Eq. (8) reduces to

$$f(\xi,\eta\to0)\sim\frac{1}{\sqrt{2\pi}}+\frac{2\eta\xi}{\pi(1-\xi^2)^{1/2}}\ . \tag{9}$$

Indeed, this function is independent of ξ when $\eta=0$. For constant positive η, the profiles of $f(\xi,\eta)$ are sharply peaked at $\xi=1$, as determined by the leading behavior of $\simeq1/\sqrt{1-\xi}$. For $\xi\to-1$, however, the probability decays exponentially as $\exp(-\eta^2/1+\xi)$ [see Fig. 4(a)]. Note also that the area of the constant η profiles is proportional to $\exp(-\eta^2/2)$, as expected. For fixed nonzero ξ, the profiles of $f(\xi,\eta)$ are peaked at a nonzero value of η that depends on ξ [Fig. 4(b)]. More surprisingly, note

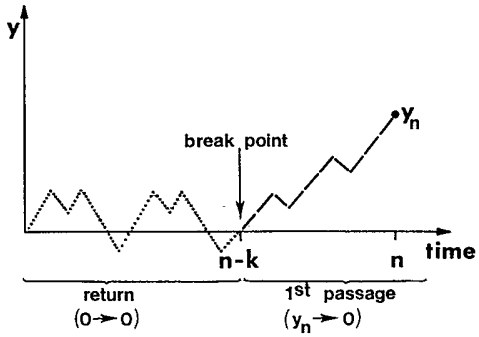

FIG. 3. Space-time representation of a random-walk path that contributes to $\mathcal{P}_n(y,n_+)$. This trajectory is decomposed into a "return" portion $(\cdots)$ and a first-passage portion $(---)$, which are separated by the break point at time step $n-k$.

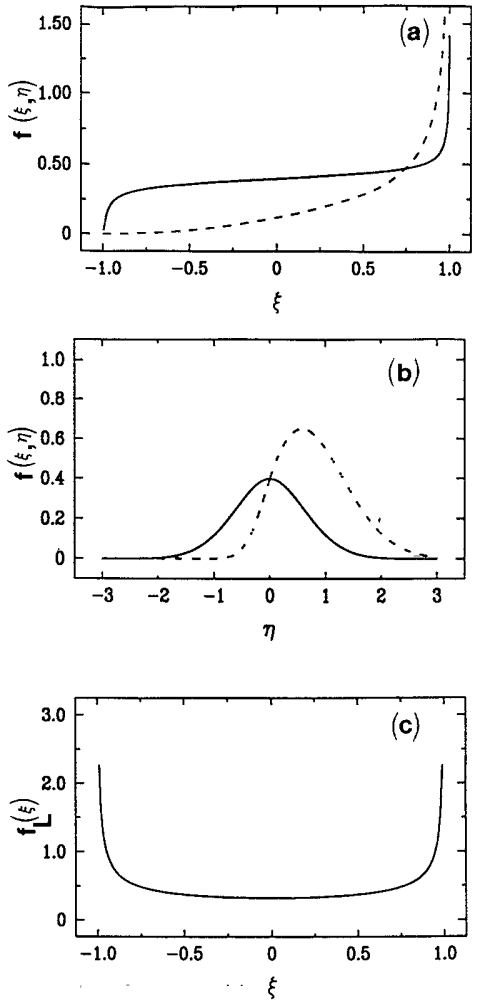

FIG. 4. Profiles of the two-dimensional probability distribution in split flow for (a) fixed η, i.e., $f(\xi,\eta=\text{fixed})$, with the cases $\eta=0.1$ (solid) and $\eta=1.0$ (dashed) shown; (b) fixed ξ, i.e., $f(\xi=\text{fixed},\eta)$, with the cases $\xi=0$ (solid) and $\xi=0.8$ (dashed) shown; (c) the arcsine law that gives the longitudinal probability distribution $f_L(\xi)$.

that the area of the profiles for fixed ξ increases as ξ increases, as required by the arcsine law.

The longitudinal probability distribution is obtained by integrating Eq. (8) over η and it gives the arcsine law [7]:

$$f_L(\xi)\sim\frac{1}{\pi(1-\xi^2)^{1/2}}\ . \tag{10}$$

In addition to being bimodal, the distribution is singular at the extrema $|\xi|=1$. Thus the split-flow velocity field, which corresponds to the case $\beta=0$ in power-law shear flow, gives rise to a probability distribution with an extreme degree of bimodality [Fig. 4(c)].

IV. LINEAR SHEAR FLOW

A well known, and exactly soluble [1–3] limit of power-law shear is the case of linear shear flow. Here we present an alternative method of solution for the discrete version of diffusion in linear shear that provides useful insights into the nature of the resulting longitudinal motion.

We define the discrete limit of linear shear flow as a random walk that moves from (x_k,y_k) to $(x_k+v_x(y_k+\epsilon_k),y_k+\epsilon_k)$ at the kth step. Here ϵ_k is a random variable that describes the individual transverse hop at the kth step and is governed by the time-independent probability distribution $p_y(\epsilon_k)$. Since $v_x(y_k)=v_0y_k$ in linear shear flow, the two-dimensional displacement after n steps can be written as

$$\begin{aligned}(x_n/v_0,y_n)&=(y_1+y_2+\cdots+y_n,\epsilon_1+\epsilon_2+\cdots+\epsilon_n)\ ,\\ &=(\epsilon_1+(\epsilon_1+\epsilon_2)+\cdots\\ &\quad+(\epsilon_1+\cdots+\epsilon_n),\epsilon_1+\epsilon_2+\cdots+\epsilon_n)\ ,\\ &=\epsilon_1(n,1)+\epsilon_2(n-1,1)+\cdots+\epsilon_n(1,1)\ .\end{aligned} \tag{11}$$

To analyze this sum, it is helpful to reverse the order of the ϵ_k. Since their distribution is independent of time, this redefinition does not affect the resulting two-dimensional distribution. Consequently, we may write the displacement after n steps as

$$(x_n,y_n)=\epsilon_1(v_0,1)+\epsilon_2(2v_0,1)+\cdots+\epsilon_n(nv_0,1)\ . \tag{12}$$

According to this expression, the longitudinal displacement in linear shear flow is equivalent to a one-dimensional random walk in which the magnitude of the kth step is simply proportional to k. This fundamental relation is the key that allows us to obtain the full two-dimensional probability distribution in linear shear flow by elementary methods.

For this purpose, we introduce the structure function [11]

$$\Gamma_n(\theta)=\sum_{\mathbf{r}}P_n(\mathbf{r})\exp(i\mathbf{r}\cdot\theta)\ , \tag{13}$$

where $P_n(\mathbf{r})$ is the probability that an n-step random walk is at $\mathbf{r}$. According to the convolution theorem,

$$\Gamma_n(\theta)=\prod_{k=1}^{n}\lambda_k(\theta)\ , \tag{14}$$

where $\lambda_k(\theta)$ is the single-step structure function,

$$\lambda_k(\theta)=\sum_{\mathbf{r}}p_k(\mathbf{r})\exp(i\mathbf{r}\cdot\theta)\ , \tag{15}$$

and $p_k(\mathbf{r})$ is the single-step probability distribution at the kth time step. Our discussion has thus far been applicable to any distribution of the ϵ_k, and we now restrict the discussion to the special case of a symmetric random walk in the y direction. Thus at the kth step, the random walk moves by an amount $\pm(kv_0,1)$, each with probability $\frac{1}{2}$ (Fig. 5). Therefore, the corresponding single-step structure function is $\lambda_k(\theta_x,\theta_y)=\cos(k\theta_x+\theta_y)$. Evaluating the product in Eq. (14) gives the structure function

$$\begin{aligned}\Gamma_n(\theta)&=\cos(v_0\theta_x+\theta_y)\\ &\quad\times\cos(2v_0\theta_x+\theta_y)\cdots\cos(nv_0\theta_x+\theta_y)\ .\end{aligned} \tag{16}$$

Moments of the probability distribution can be found by appropriate differentiation of the structure function, Eq. (13). This calculation gives

$$\langle x_n^j y_n^k\rangle=i^{j+k}\frac{\partial^{j+k}\Gamma_n(\theta)}{\partial\theta_x^j\partial\theta_y^k}\bigg|_{\theta=0}\ . \tag{17}$$

From this, we find, for example,

$$\langle x_n^2\rangle\sim v_0^2n^3/3,\quad\langle x_ny_n\rangle\sim v_0n^2/2\ . \tag{18}$$

Thus the mean-square longitudinal displacement in linear shear grows as t^3, and perhaps less well appreciated, the longitudinal and transverse displacements are coupled so that cross correlations are nonzero.

Finally, the probability distribution $P_n(\mathbf{r})$ can be easily extracted from Eq. (16) by the standard procedure of expanding this expression for small θ_x and θ_y, reexponentiating, and then performing an inverse Fourier transform of the result. This gives the long-time limit of the probability distribution as

$$\begin{aligned}P_n(x,y)&\sim\frac{\sqrt{3}}{\pi v_0n^2}\exp(-y^2/2n)\\ &\quad\times\exp[-6(x-\langle v\rangle n)^2/v_0^2n^3]\ ,\end{aligned} \tag{19}$$

where $\langle v\rangle=v_0y/2$ is the average velocity of the trans-

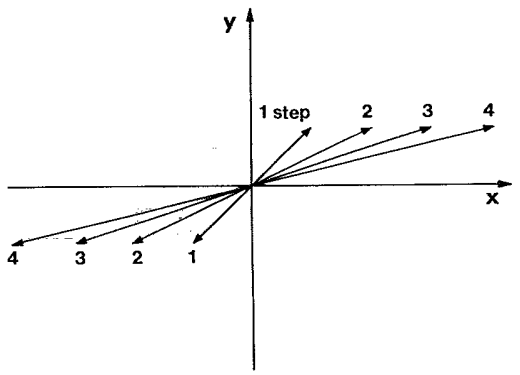

FIG. 5. Sequence of single-step distributions in linear shear flow.

verse coordinate in the range $[0,y]$. For fixed y the probability profile is a Gaussian function that is peaked at $x=\langle v\rangle n$ and whose width grows as $t^{3/2}$.

An advantageous consequence of our method of solution is that it exposes the basic equivalence between convection diffusion in linear shear flow and a temporally inhomogeneous random-walk process in which the step length grows linearly in time. In the continuum limit, this leads to a diffusive process with a time-dependent diffusion coefficient $D(t)=\Delta x(t)^2/\Delta t=D(v_0t)^2$. Consequently, the longitudinal probability distribution obeys

$$\frac{\partial P_L(x,t)}{\partial t}=D(v_0t)^2\frac{\partial^2 P_L(x,t)}{\partial x^2}\ . \tag{20}$$

The solution to this equation is the Gaussian $f_L(\xi)\sim\sqrt{3/2\pi}\exp(-3\xi^2/2)$ [following the notations of Eqs. (3) and (4)], a result that also follows directly from Eq. (19). Since the distribution is a pure Gaussian, the large-distance tail of this distribution, which is predicted by the argument given in Sec. II, is actually valid over the entire range of ξ.

V. EFFECTIVE-VELOCITY APPROXIMATION

Since the exact expression for $P_L(x,t)$ is bimodal for $\beta=0$ and unimodal for $\beta=1$, the distribution must change between these two shapes as β varies between 0 and 1. We now wish to determine the location and the nature of this shape transition. To derive the functional form of $P_L(x,t)$ for general β, we introduce the following effective-velocity approximation [6]. We hypothesize that at a fixed value of $y=y_0$, the probability distribution $P(x,y_0,t)$ is given by the Gaussian form of Eq. (19), but with the average longitudinal velocity $\langle v\rangle$ now proportional to y^β. This may be realized by allowing the parameter v_0 to acquire a dependence on y, which is determined by $\langle v(y)\rangle\propto v_0(y)y=y^\beta$, or

$$v_0(y)\propto y^{\beta-1}\ . \tag{21}$$

With this hypothesis, Eq. (18) predicts that at fixed $y=y_0$, the longitudinal dispersion $\delta x(y_0)$ is proportional to $y_0^{\beta-1}$, a result that we have also confirmed numerically. Thus, for $0\le\beta<1$, the relative longitudinal width decreases with y_0, although the velocity increases in y_0.

In our effective-velocity approximation, we use the two-dimensional Gaussian distribution, Eq. (19), together with the velocity given in Eq. (21), and integrate over the transverse coordinate to obtain an approximate form for $P_L(x,t)$. In performing these steps, it is convenient to reexpress the integrand in terms of the scaled coordinates ξ and η and use symmetry of the integrand in η to write the integral over positive η only. This computation gives (dropping all irrelevant numerical factors)

$$f_L(\xi)\sim\int_{\eta=0}^{\infty}d\eta\,\eta^{1-\beta}\exp(-2\eta^2)\exp(-6\xi^2\eta^{2-2\beta})\times\cosh(6\xi\eta^{2-\beta})\ . \tag{22}$$

For large ξ, the asymptotic behavior of the integral is determined by the maximum of the function in the exponential at $\eta_0=\xi^{1/\beta}$. Performing the integral by the Laplace method yields the large-distance behavior

$$f_L(\xi)\sim\exp(-\xi^{2/\beta})\ , \tag{23}$$

which gives the same shape exponent as that predicted by the naive argument of Sec. II.

The transition point between bimodality and unimodality can be determined by evaluating the second derivative of Eq. (22) at $\xi=0$. Omitting irrelevant factors, this calculation yields

$$\left.\frac{\partial^2}{\partial\xi^2}f_L(\xi)\right|_{\xi=0}\propto\int_{\eta=0}^{\infty}d\eta\exp(-2\eta^2)(3\eta^{5-3\beta}-\eta^{3-3\beta})\propto\Gamma\left[\frac{4-3\beta}{2}\right]\left[\frac{8}{9}-\beta\right]\ , \tag{24}$$

where the last expression is valid only for $\beta<\frac{4}{3}$. For $\beta>\frac{4}{3}$, the second derivative of $f_L(\xi)$ at $\xi=0$ diverges, indicative of a cusp in the distribution function at the origin. The effective-velocity approximation therefore predicts that the transition point between unimodality and bimodality occurs at $\beta_c=\frac{8}{9}$, compared to our numerical estimate $\beta_c=\frac{3}{4}$ (see below).

Similar qualitative results are obtained if we use an effective-velocity approximation with the two-dimensional distribution of split flow as the basis for writing the general β distribution. In this case, the amplitude of the velocity v_0 must now acquire the y dependence $v_0(y)=y^\beta$, in order to obtain the appropriate magnitude of the longitudinal velocity at $y=y_0$. Using this result, and following step by step the reasoning that led to Eq. (22), we obtain an expression for $f_L(\xi)$ that is characterized by a shape exponent $\delta=2/\beta$ and the longitudinal dispersion $\delta x(y_0)\sim y_0^{\beta-1}$, in agreement with the results obtained by using the distribution of linear shear as the basis for the effective-velocity approximation. The analytic expression that determines the critical value of β is complicated and numerically we estimate that $\beta_c\approx0.5$. Thus both effective-velocity approximations predict qualitatively similar properties for the longitudinal distribution.

VI. EXACT ENUMERATION OF THE PROBABILITY DISTRIBUTION

To test our predictions about the nature of the longitudinal probability distribution, we now present the results of a numerical exact enumeration [12] in power-law shear flow. At the start of the enumeration, there is a unit probability at the origin, and we evolve the probability distribution according to the recursion relation

$$P_{n+1}(x,y)=\sum_{y'=y\pm1}\tfrac{1}{2}P_n(x-v_x(y'),y')\ . \tag{25}$$

This evolution process takes into account both transverse diffusion and longitudinal convection. In the case of a noninteger value for the velocity, this recursion formula would lead to the probability being propagated to positions between lattice sites. When this occurs, the interstitial probability element is split longitudinally between the

two nearest-neighbor sites, with the relative weight of each component ensuring that the correct average displacement occurs.

Over the temporal range of our enumeration (up to 128 time steps), the longitudinal distribution is a scaling function of ξ to a high degree of accuracy. This verification of scaling thus excludes the possibility that the longitudinal distribution could undergo a unimodal to bimodal transition as a function of time. Consequently, the numerical determination of β_c is relatively unambiguous. In Fig. 6(a) we plot the scaled probabilities versus the scaled coordinate for various values of β. At $\beta=1$, the distribution is a Gaussian, and as β is decreased the distribution develops broader shoulders. As $\beta\to\beta_c$, the distribution becomes flat at the maximum, indicative of the vanishing of the second derivative at $\xi=0$. Numerically, we find the critical value of β to be 0.75 ± 0.01. As β is decreased beyond this point, the bimodality of the distribution becomes more pronounced, and ultimately a singularity develops at $|\xi|=1$ when $\beta=0$. Qualitatively, these features mirror our theoretical predictions.

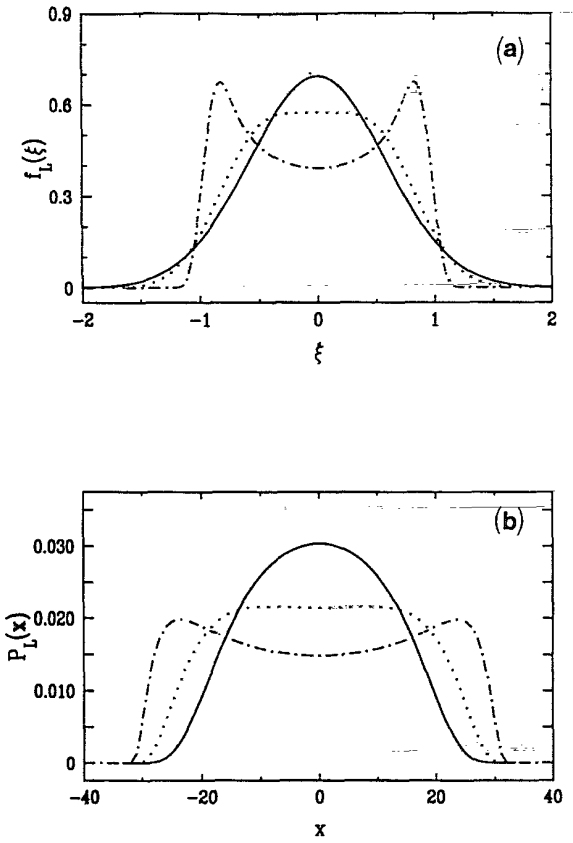

FIG. 6. (a) Exact enumeration results for the scaling function $f_L(\xi)$ vs ξ in power-law shear flow at 64 time steps for (i) $\beta=0.25$ (dashed), (ii) $\beta=0.75$ (dotted), and (iii) $\beta=1.0$ (solid). (b) Exact enumeration results at 32 time steps for $P_L(x,t)$ vs x in the flow field given by Eq. (27) for a power-law fluid for the cases of (i) $n=\frac{1}{14}$ (dashed), (ii) $n=\frac{1}{7}$ (dotted), and (iii) $n=\frac{1}{4}$ (solid).

VII. AN APPLICATION TO NON-NEWTONIAN FLUIDS

A potential application of the abstract power-law shear flow problem is to the Brownian motion of a dynamically neutral tracer particle in a class of non-Newtonian fluids, where the shear (assumed to be along the y direction) and the force along x, τ_{xy}, are related by

$$\tau_{xy}\propto\left[\frac{dv_x}{dy}\right]^n . \tag{26}$$

Thus the exponent n quantifies the nonlinearity of the fluid [13]; for $n=1$, one recovers a Newtonian fluid, while if $n\neq1$, one has a "power-law" fluid. Under the application of a shear, a power-law fluid develops a flow field in which the longitudinal velocity has a functional dependence on the transverse coordinate that qualitatively resembles that of power-law shear flow. Hence, we might expect that tracer motion in a non-Newtonian fluid will exhibit the same rich spectrum of behavior as in power-law shear. In particular, by varying the exponent n, or equivalently, by varying external parameters of the flow itself, it should be possible to obtain both bimodal and unimodal distributions of longitudinal displacements for tracer particles.

For example, consider the case of plane Couette flow. For two parallel planes at $y=-L$ and L moving at velocities $-v_0$ and $+v_0$, respectively, along the x direction, the steady-state velocity profile is [13]

$$v_x(y)=v_0\,\mathrm{sgn}(y)\frac{\lambda^m-(\lambda|y|)^m}{\lambda^m-(\lambda-L)^m} , \tag{27}$$

where $m=1+1/n$, and λ is a constant with the dimension of a length whose value depends on details such as the external pressure gradient, the velocity at the boundary, etc. Qualitatively, this velocity profile is very similar to that in power-law shear flow (Fig. 7), and there is a similar correspondence between the probability distributions [Fig. 6(b)]. The analogy with power-law shear flow should hold as long as $\sqrt{Dt}<L$, as the influence of the transverse boundaries of the system are irrelevant within this temporal range. Our enumeration for the case $\lambda=L=32$ after 32 time steps exhibits a transition from bimodality at small n to unimodality when $n_c\approx\frac{1}{7}$. This transition can also be produced by fixing the value of n

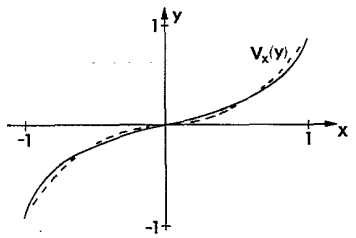

FIG. 7. Comparison of the velocity profiles of power-law shear flow with $v_0=1$ and $\beta=0.45$ (dashed), and of a power-law fluid in Couette flow [Eq. (27)], with $v_0=L=1$, $\lambda=4$, and $n=\frac{1}{9}$ (solid).

and varying λ. For example, the situation where $n=\frac{1}{7}$ and $\lambda \gg L$ corresponds to linear shear, where the probability distribution is unimodal. Conversely, the case where $n=\frac{1}{7}$ and $\lambda < 32$ should lead to a bimodal distribution. Thus the transition can be obtained either by tuning n, the nonlinearity exponent of the fluid, or by tuning λ, which can be achieved by experimentally controllable parameters contained in λ. Therefore, the unimodal to bimodal transition is an aspect of transport in non-Newtonian fluids, which should be amenable to experimental observation.

VIII. CONCLUSIONS

We have elucidated some unusual features of the motion of dynamically neutral tracer particles that are carried by a power-law shear flow, where $\mathbf{v}(x,y)=v_0|y|^{\beta}\mathrm{sgn}(y)\hat{\mathbf{x}}$. Our main result is that the probability distribution of longitudinal displacements, $P_L(x,t)$, is bimodal for small β and unimodal for larger β. From a practical viewpoint, this result may apply to tracer motion in a non-Newtonian fluid. The existence of this transition follows from consideration of the special cases $\beta=0$ (split flow), where the distribution is bimodal, and $\beta=1$ (linear shear flow), where the distribution is unimodal. For these cases, we also obtained the exact expressions for the two-dimensional probability distributions.

These results serve as a starting point for writing an effective-velocity approximation for $P_L(x,t)$ for general β, an approach which appears to capture the essential mechanism underlying the unimodal to bimodal transition. This mechanism can be appreciated by viewing the full longitudinal distribution $P_L(x,t)$ as a superposition of longitudinal distributions for each layer with fixed $y=y_0$. Each component-layer distribution is characterized by its average position $\langle x(y)\rangle$, its width $\delta x(y)$, and its weight $e^{-y^2/t}$. The competition between these three factors, as the component distributions for different values of y are superposed, governs the shape of $P_L(x,t)$.

For the case of small β, $\langle x(y)\rangle$ rapidly increases as a function of y, while $\delta x(y)$ is decreasing in y. These features lead to a bimodal form of $P_L(x,t)$ when the superposition of layer distributions is performed. On the other hand, for $\beta \lesssim 1$, $\langle x(y)\rangle$ increases nearly linearly in y, while $\delta x(y)$ is nearly independent of y. Consequently, the superposition of distributions for each layer should lead to a unimodal shape. The effective-velocity approximation involves taking either the two-dimensional distribution of split flow or linear shear flow, and incorporating a physically motivated functional form for $\langle x(y)\rangle$ that concomitantly determines $\delta x(y)$. The competition between these two quantities when the superposition over all layers is performed provides a simple and reasonably accurate description of the unimodal to bimodal transition.

ACKNOWLEDGMENTS

We thank F. Leyvraz for numerous useful discussions during the course of this work. We also gratefully acknowledge financial support through grants from the ARO and NSF (S.R.) and NSF and PRF (D.bA.).

[1] G. K. Batchelor, J. Fluid Mech. **95**, 369 (1979).
[2] R. T. Foister and T. G. M. Van De Ven, J. Fluid Mech. **96**, 105 (1980).
[3] R. Mauri and S. Haber, SIAM J. Appl. Math. **46**, 49 (1986).
[4] G. Matheron and G. de Marsily, Water Resour. Res. **16**, 901 (1980).
[5] J.-P. Bouchaud, A. Georges, J. Koplik, A. Provata, and S. Redner, Phys. Rev. Lett. **64**, 2503 (1990).
[6] D. ben-Avraham, F. Leyvraz, and S. Redner, Phys. Rev. A **45**, 2315 (1992).
[7] W. Feller, *An Introduction to Probability Theory and its Applications* (Wiley, New York, 1968), Vol. 1, Chap. 3.
[8] P. Pincus, Macromolecules **9**, 386 (1976).
[9] P.-G. de Gennes, *Scaling Concepts in Polymer Physics* (Cornell University Press, Ithaca, 1979).
[10] M. E. Fisher, J. Chem. Phys. **44**, 616 (1966).
[11] G. H. Weiss and R. J. Rubin, Adv. Chem. Phys. **52**, 363 (1983).
[12] S. Havlin and D. b.-Avraham, Adv. Phys. **36**, 695 (1987).
[13] R. B. Bird, R. C. Armstrong, and O. Hassager, *Dynamics of Polymeric Liquids* (Wiley, New York, 1977), Vol. 1, Chap. 5.